Intraoperative subcortico-cortical evoked potentials of the visual pathway under general anesthesia

Boex, Colette; Goga, Cristina; Bérard, Nadia; Al Awadhi, Abdullah; Bartoli, Andréa; Meling, Torstein; Bijlenga, Philippe Alexandre Pierre; Schaller, Karl Lothard

How to cite

BOEX, Colette et al. Intraoperative subcortico-cortical evoked potentials of the visual pathway under general anesthesia. In: Clinical Neurophysiology, 2021, vol. 132, n° 7, p. 1381–1388. doi: 10.1016/j.clinph.2021.02.399

This publication URL: https://archive-ouverte.unige.ch/unige:158225
Publication DOI: 10.1016/j.clinph.2021.02.399

Clinical Neurophysiology 132 (2021) 1381–1388

Contents lists available at ScienceDirect

Clinical Neurophysiology

journal homepage: www.elsevier.com/locate/clinph

Intraoperative subcortico-cortical evoked potentials of the visual pathway under general anesthesia

Colette Boëx [a,b,*], Cristina Goga [c], Nadia Bérard [a], Abdullah Al Awadhi [b,c], Andrea Bartoli [c], Torstein Meling [b,c], Philippe Bijlenga [b,c], Karl Schaller [b,c]

[a] Department of Neurology, Geneva University Hospitals, Geneva, Switzerland
[b] Faculty of Medicine, University of Geneva, Geneva, Switzerland
[c] Departement of Neurosurgery, Geneva University Hospitals, Geneva, Switzerland

ARTICLE INFO

Article history:
Accepted 9 February 2021
Available online 9 April 2021

Keywords:
Neuromonitoring
Visual evoked potentials
Optic radiations

HIGHLIGHTS

- Optic tract mapping was found feasible.
- Early latency waveform P1 was in agreement with the conduction velocity of myelinated fibers.
- Middle latency waveform P2 could be attributed to activation of secondary visual cortices.

ABSTRACT

Objective: To assess whether intraoperative subcortical mapping of the visual pathways during brain surgeries was feasible.
Methods: Subcortico-cortical evoked potentials (SCEPs: 30 stimulations/site, biphasic single pulse, 1.3 Hz, 0.2 ms/phase, maximum 10 mA; bipolar probe) were measured in 12 patients for stimulation of the optic radiation, Meyer's loop or optic nerve. Recorded sites were bilateral central, parietal, parieto-occipital, occipital (subdermal scalp electrodes, 5–4000 Hz). The minimum distances from the stimulation locations, i.e. the closest border of the resection cavity to the diffusion tensor imaging based visual pathways, were evaluated postoperatively (smallest distance across coronal, sagittal and axial planes).
Results: Stimulation elicited SCEPs when the visual tracts were close (≤4.5 mm). The responses consisted of a short (P1, 3.0–5.6 ms; 8/8 patients) and of a middle (P2, 15–21.6 ms; 3/8 patients) latency waveforms. In agreement with the neuroanatomy, ipsilateral occipital responses were obtained for temporal or parietal stimulations, and bi-occipital responses for optic nerve stimulations.
Conclusions: For the first time to our knowledge, intraoperative SCEPs were observed for stimulations of the optic radiation and of Meyer's loop. Short latency responses were found in agreement with fast conduction of the visual pathway's connecting myelinated fibers.
Significance: The mapping of the visual pathways was found feasible for neurosurgeries under general anesthesia.

1. Introduction

Neurosurgery of the temporal lobe poses a risk of lesion of Meyer's loop, which is a frequent cause of quadrantanopia in epilepsy surgeries (Jeelani et al., 2010, Yeni et al., 2008) or in other temporal lobe surgeries (Faust and Vajkoczy, 2016). Furthermore, resection of parietal, parieto-temporal, parieto-occipital or occipital lesions exposes to a risk of visual impairment, because of their proximity to the optic radiation or to the visual cortex, and may result in homonymous hemianopia (Zhang et al., 2006). Hemianopia is a debilitating deficit, causing patients to become unable to read or drive (Goodwin, 2014).

Identification of Meyer's loop and the optic tract by diffusion tensor imaging[1] (DTI) and visualization by neuro-navigation were introduced to improve the extent of temporal resection while minimizing the risk of leaving tumor remnants behind or of unsatisfac-

* Corresponding author at: Department of Neurology, Geneva University Hospitals, Geneva, Switzerland.
E-mail address: Colette.Boex@hcuge.ch (C. Boëx).

[1] DTI: diffusion tensor imaging.

https://doi.org/10.1016/j.clinph.2021.02.399
1388-2457/

tory outcomes following temporal lobe epilepsy surgery (Chen et al., 2009, Yogarajah et al., 2009). DTI allows the identification of lesion-induced displacements of the optic radiation. Thereby, it helps to decide the best surgical approach and avoid lesions of these fibers (Faust and Vajkoczy, 2016).

Visual evoked potentials[2] (VEPs) are becoming a standard tool in the field of intraoperative neuromonitoring, thanks to their capacity to provide warnings during the manipulation of visual cortices or pathways (Gutzwiller et al., 2018, Kodama et al., 2010, Sasaki et al., 2010). Nevertheless, a visual mapping technique with a "rule of thumb", similar to the one used for corticospinal tract motor mapping (Raabe et al., 2014, Sala and Lanteri, 2003), is still missing. Such a continuous dynamic mapping technique could contribute to increase the resection safety of brain lesions near visually eloquent areas.

Subcortical visual pathways can be identified by the application of direct subcortical stimulation, as performed for visual tracts in awake surgeries (Duffau, 2011, Duffau et al., 2004, Gras-Combe et al., 2012, Mazerand et al., 2017). In the context of general anesthesia, the use of subcortico-cortical evoked potentials[3] (SCEPs) obtained in response to the electrical stimulation of the visual pathways could serve the same purpose. So far, SCEPs have been performed for language monitoring, in particular for the stimulation of the arcuate fasciculus (Mandonnet et al., 2016, Yamao et al., 2014, Yamao et al., 2017). However, assessment of the visual system under general anesthesia has only been reported with intraoperative stimulation of the optic nerve (Benedicic and Bosnjak, 2011). The aim of the present study is to evaluate the feasibility of direct subcortical stimulation of visual pathways in patients under general anesthesia. The optic nerve, Meyer's loop and the optic radiation were directly stimulated intraoperatively, and the SCEPs associated with the stimulations were recorded and analyzed. For the late patients, preoperative imaging of the visual pathways using T1W MRIs were displayed into the neuronavigation system (Brainlab), with DTI-based fiber tractography (Brainlab Elements platform).

2. Methods

The prospective study was performed according to the ethical guidelines of the Declaration of Helsinki. The study was approved by the Ethics Committee of Geneva (CE no 12-246).

2.1. Patients

Eighteen patients agreed to participate and signed the dedicated consent form. Stimulation of the visual pathway was actually performed by the operator in 12 patients (7 females, 5 males, mean age: 51.5 years -y-, standard deviation: 15.2 y; Table 1). Stimulation was not attempted in 6 patients for whom the operator was not involved directly in the study. All 12 patients underwent microsurgical resections of intrinsic or extrinsic cerebral lesions (6 gliomas, 3 meningiomas, 1 arteriovenous malformation, 1 cavernoma, 1 hippocampal sclerosis) under general anesthesia. Lesion locations were either temporal or temporo-occipital (n = 5), parietal or temporo-parietal (n = 4), or sphenoidal (n = 3); all of them required dissection adjacent to a part of the visual pathway.

Visual fields were assessed preoperatively and at 1-month post-surgery using Goldmann perimetry (Octopus, Haag-Streit, Bern, CH) in the Ophthalmology Department of the Geneva University Hospitals. Possible changes in the visual field were categorized as (1) discrete quadrantanopia (i.e. new diffuse deterioration < 2 dB), (2) complete quadrantanopia or (3) hemianopia.

2.2. Stimulation and evoked potentials (VEPs)

SCEPs were performed using a bipolar probe with isolated wires (HV, stimflex 522017, inomed Medizintechnik GmbH) for direct subcortical stimulation of the visual pathways (biphasic waveforms, 0.2 ms per phase, repeated at a 1.3 Hz rate). The stimulation intensity started at 10 mA, at maximum, for optic radiation and Meyer's loop stimulation. The stimulation was limited to low intensities [2.5–3.5 mA], for optic nerve stimulation, the stimulation being in direct contact with the optic nerve. The stimulation duration for this very novel technique was also limited and stopped usually once response observed. A limitation on the voltage of the current sources was applied to avoid stimulation artifacts (when the stimulation probe is in the air, the current source sends the maximum voltage made available by the system; once it is in contact with the brain, the current requested by the user is delivered and the voltage reduces according to the impedance of the brain interface). SCEPs were recorded bilaterally using central, parietal, parieto-occipital, and occipital subcutaneous corkscrew electrodes (bandpass filtering: 5–4000 Hz). One SCEP was usually obtained averaging 30 responses per site of stimulation. Cz was the reference electrode, with the ground electrode made of linked A1 and A2 (International 10–20 EEG system). During the preoperative set-up, the electrode cables were all wound together to, once again, help reduce the stimulation artifacts. The intraoperative neuromonitoring systems used were either the ISIS IOM system (inomed Medizintechnik GmbH) or the NIM-ECLIPSE system (Medtronic).

During surgery, standard flash visual evoked potentials (VEPs) were performed (recordings O1, O2, reference Cz, ground A1-A2; 2–400 Hz bandpass filtering; maximum 60 repetitions per VEP, duration of exposure per repetition < 10 ms, maximum 6000Lx, repetitions < 1 Hz, with simultaneous electroretinogram recordings) (Gutzwiller et al., 2018). The light-emitting diodes, placed over the patients' eyes, were carefully protected from scialytic operating room lamps and from the microscope light with a film of aluminium, separated from the patient by a soft tissue.

2.3. Imaging techniques

Computation of tumor and possible residual tumor volumes were performed with pre- and early postoperative (<48 h) MRIs (Siemens Trio 3.0 T scanner). It was conducted by a trained neurosurgeon (C.G.) using a quantitative, semi-automated volumetric tool (Smart Brush Tool, Brainlab Elements Cranial, Brainlab). For non-enhancing lesions, the preoperative tumor volume was defined on 3D precontrast T2/FLAIR sequences. The possible residual tumor volumes were computed on the postoperative 3D T2/FLAIR sequences by segmenting the area of residual tissue abnormality in all planes and excluding the resection cavity. The T1-weighted gadolinium-enhanced and non-enhanced images were compared to exclude post-operative blood products from volume calculations. The extent of resection was calculated as previously described (Smith et al., 2008). For enhancing lesions, 3D T1-weighted MPRAGE gadolinium-enhanced slices were used instead of the 3D precontrast T2/FLAIR sequences.

Distances from the visual pathway to the resection cavity were computed postoperatively. Diffusion tractography (DTI) sequences were performed with, for non-enhancing lesions, postoperative 3D with T2/FLAIR sequences, and for enhancing lesions, with single-shot spin echo planar imaging fused 3D T1-weighted MPRAGE gadolinium-enhanced slices. The DTI sequences were performed with the following parameters: 30 gradient directions in axial

[2] VEPs: Visual evoked potentials.
[3] SCEPs: Subcortico-cortical evoked potentials.

Table 1
Characteristics of patients, lesions, stimulations, and responses.

Patients	Lesion location	Side	Pathology	Volume Pre/post (cm^3)	Targeted site of stimulation	Stimulation (mA)	Distance to the visual pathway (mm)	P1 waveform : location, latency, voltage	P2 waveform : location, latency, voltage	Anatomical locations of responses	Intraop. VEP changes	Extent of resection (%)	Neuro-navigation with DTI(if not N)	Visual field changes6 weeks postop.
P12	Parietal (opercula)	L	Cavernoma	2.5/0.0	L optic radiation	7.0	9.0	None	None	NA	None	100	DTI	None
P2	Temporo-occipital	R	Glioblastoma	9.7/0.8	R optic radiation	10	7.4	None	None	NA	None	92	N	None
P11	Temporal	L	Glioblastoma	6.8/0.0	L optic radiation	5.0	6.5	None	None	NA	None	100	DTI	Discrete homonymous quadrantanopia (R eye > L eye)
P1	Temporal	L	Hippocampal sclerosis	NA	L Meyer's loop	3.0	6.2	None	None	NA	None	100	N	None
P13	Temporal	L	Ganglioglioma	3.5/0.0	L Meyer's loop, optic radiation	**7.0**	**4.5**	**PO7 > O1, 2.4 ms, 2.5 µVpp**	None	L parieto-occipital L occipital	NC	100	DTI	Homonymous quadrantanopia @ 2 weeks
P9	Temporo-occipital	L	Arteriovenous malformation	2.7/0.0	L optic radiation	**5.0**	**2.1**	**O1 > PO7, 5.4 ms, 2.2 µVpp**	**O1 > PO7, 21.6 ms, 2.4 µVpp**	L occipital L parieto-occipital	L permanent decrease (R eye)	100	DTI	Discrete heteronymous quadrantanopia (R eye)
P5	Temporo-parietal	R	Glioblastoma	30.5/ 9.2	R optic radiation	**8.0**	**0.0**	**O2, 3.0 ms, 0.8 µVpp**	**O2, 15.0 ms, 4.5 µVpp**	R occipital (parietal not recorded)	None	70	N	NA before second surgery
P6	Temporo-parietal	R	Glioblastoma	127.3/0	R optic radiation	**8.0**	**0.0**	**O2 > PO8, 3.6 ms, 1.5 µVpp**	**O2 > PO8, 17.0 ms, 18.0 µVpp**	R occipital, R parieto-occipital	R temporary decrease	100	N	Homonymous hemianopia
P15	Parietal	R	Glioblastoma	15.3/0.0	R optic radiation	**7.0**	**0.0**	**O2 > P4, 2.8 ms, 2.8 µVpp**	None	R parieto-occipital R occipital	None	100	DTI	Deterioration of hetero- to homonymous hemianopia
P10	Sphenoidal	L	Meningioma	NA	L optic nerve	**3.0**	**0.0**	**O1 > O2, 3.8 ms, 3.5 µVpp**	None	Occipital bilaterally	NC	<90*	NA	Heteronymous quadrantanopia
P17	Sphenoidal	R	Meningioma	NA	L optic nerve	**3.5**	**0.0**	**O1 > O2, 5.6 ms, 1.0 µVpp**	None	Occipital bilaterally	None	100*	NA	None
P18	Sphenoidal	L	Meningioma	NA	R optic nerve	**2.5**	**0.0**	**O2 > O1 > PO8, 4.2 ms, 2.0 µVpp**	None	Occipital bilaterally	None	100*	NA	None

Location of the lesion, side of the lesion (L: left, R: right), pathology of the lesion, volume of the lesion preoperatively (Pre) and postoperatively (post, NA: not available); location of the stimulation, maximum stimulation intensity applied (mA), minimum distance between the stimulation site and the visual pathway (mm), P1 and P2 waveform locations of the subcortico-cortical evoked potentials (SCEPs) according to the International 10–20 EEG system (O1, O2, PO7, PO8), waveform latencies (ms), and maximum peak-to-peak voltages (µVpp); anatomical locations of the SCEPs, intraoperative visual evoked potential (VEP) changes (NC: not contributive), percentage of resection extension in reference to the preoperative lesion volume, * described by a radiologist, and postoperative visual field changes. Neuronavigation with diffusion tensor imaging (DTI) or not (N). Shaded cells: NIM-ECLIPSE monitoring system; white cells: ISIS IOM system. NA: not available, NC: not contributive.

plane and *b* values at 0 and 1000 s/mm^2; FOV 230 mm × 230 mm; voxel size 1.8 mm × 1.8 mm × 2.0 mm, flip angle 90°, echo time TE 82 ms, repetition time TR 8200 ms. The visual pathways were computed using the Fibertracking tool of the Brainlab Elements Cranial (Brainlab AG). Seeding was performed using the Interactive Brush function. Two regions of interest (ROI) were placed at the level of the lateral geniculate nucleus and in the occipital white matter. The fractional anisotropy threshold was set to 0.1, minimum fiber length was set to 100 mm and maximal angulation to 80°. The "remove" function was used to edit the rendered fiber tract and remove the aberrant fibers. The DICOM Viewer tool of the Brainlab Elements Cranial was used to visualize the reconstructed tract overlaid on the anatomical MRI images, and to measure distances. The shortest distance from the visual pathway to the closest margin of the resection cavity was estimated by calculating the mean of the minimal distances measured sequentially across axial, coronal, and sagittal slices.

For patients P9, P11, P12, P13, and P10, lesions and visual pathways were modeled as 3D objects and displayed into the surgical microscope intraoperatively, using augmented reality and the neuronavigation system (Brainlab Curve, Brainlab AG). Lesions and visual pathways were identified by DTI-based fiber tractography (Brainlab Elements platform, Brainlab AG) on preoperative imaging. Shifts of brain structures associated with cerebrospinal fluid loss and tissue resection were corrected by updating the navigation registration using signature vessel structures (Bijlenga P., personal communication). For patient P9, the precise locations of the white matter stimulation points were recorded in the neuronavigation, allowing a precise measurement of the distance to the optic radiation identified using fiber tractography.

2.4. Anesthesia

Anesthesia was induced with propofol (Schnider et al., 1998, Schnider et al., 1999) and sufentanil (Gepts et al., 1995) via target-controlled infusion. The initial concentrations were of 4.5–5.0 μg/ml for propofol and of 0.3–0.4 ng/ml for sufentanil. The concentrations were adjusted according to the patients' needs ([3.0–4.5] μg/ml propofol and [0.15–0.25] ng/ml sufentanil) during maintenance.

3. Results

Stimulation of the optic radiation was performed in 2 patients with a left temporal World Health Organization (WHO) grade IV glioblastoma (P13) or amygdala ganglioglioma (P11); one patient with a left operculo-parietal cavernoma (P12); one patient with a left temporo-occipital arteriovenous malformation (AVM, P9); one patient with a left hippocampal sclerosis (P1); and 4 patients with right WHO grade IV glioblastomas: temporo-parietal (P5, P6), parietal (P15) or occipital (P2).

For all of these patients, evoked responses were obtained in all stimulations with distances shorter than 4.5 mm relative to the optic radiation, Meyer's loop or optic nerve.

In the cases of the optic radiation stimulation, evoked responses were obtained in all stimulations with distances shorter than 4.5 mm relative to the optic radiation, with stimulation intensities in the 5 to 8 mA range (Table 1). However, no evoked response was observed for stimulations located more than 4.5 mm from the optic radiation, with stimulation intensities ranging from 5 to 10 mA. The recorded responses presented 2 different latency waveforms (Table 1): a short latency P1 response (2.4–5.4 ms) and a middle latency P2 response (15–21.6 ms). The P2 response waveforms were observed in only 3 patients for whom direct or very close (i.e. 2.1 mm) stimulations of the optic radiation were applied with stimulation intensities ranging between 5 to 8 mA. These waveforms were observed ipsilateral to the stimulation sites.

Fig. 1 illustrates the resection in patient P9 undergoing surgery for a left temporo-occipital AVM (red). In the neuronavigation, the AVM appeared overlaid in red while the optic radiation was overlaid in green, and the overlays were projected into the microscope as an augmented reality image at the time of resection. The bipolar stimulation was applied to the antero-lateral border of the resection cavity, at the end of resection, in contact with the white matter at the edge of the optic radiation model (green overlay). In this single patient, the stimulation site's distance from the segmented optic radiation (green) was intraoperatively estimated. It was found to be of 3 mm ("point#11", Fig. 1), and postoperatively found to be of 2.1 mm. Evoked potentials with P1 waveforms were observed at the left occipital and parietal cortical channels (green trace, "O1-Fz", "P7-Fz", channel misnamed were -Cz), in response to the stimulation at label "point#11". Consistent with the proximity of the resection to the left optic radiation in this patient, a temporary decrease in the amplitude of the left occipital VEP responses (left column of the top left subpart of Fig. 1; e.g. 14h16, 14h18) to the excitation of the right eye was observed during the resection, and the patient observed a discrete deterioration of their right visual field.

Fig. 2 illustrates the resection in patient P15 for a right parietal high grade glioblastoma, with intraoperative imaging of the visual pathways. MRIs were displayed into the neuronavigation system (Brainlab) with DTI-based fiber tractography, with the optic radiation overlaid in green in the augmented reality image injected into the microscope at the time of resection. At the end of resection, SCEPs were observed in responses to the bipolar stimulation ipsilaterally to the stimulation side (P1, 3.8 ms). The complete resection performed in this case, with direct contact between the lesion and the optic radiation, was associated with the deterioration of an existing heteronymous hemianopia toward a homonymous hemianopia, not detected intraoperatively using the VEPs (channel O2-Cz in Fig. 2), in the context of ischemic-hemorrhagic changes at the edges of the cavity.

A tumor remnant of a glioblastoma in direct contact with the optic radiation, confirmed by SCEPS with P1 and P2 waveforms observed in response to stimulation, required a revision surgery in patient P5 (Supplementary Fig. 1, blue arrows). The patient suffered of partial homonymous hemianopia after the second surgery. In the last case of a glioblastoma in direct contact with the optic radiation, i.e. in patient P6, the full resection was associated with a new homonymous hemianopia. The Supplementary Fig. 2 illustrates the SCEPs (blue arrows) obtained only for stimulation sites in contact with the optic radiation in patient P6.

Videos 1 and 2 illustrate the stimulation of Meyer's loop during the resection of a left temporal amygdala ganglioglioma in patient P13 (Video 1). DTI-based fiber tractography, representing Meyer's loop in pink and the optic radiation in green, was injected into the microscope as an augmented reality image. In response to the stimulation of Meyer's loop (pink), short latency P1 responses were recorded in the left occipital and parieto-occipital cortical channels ("O1-Pz", "PO7-Pz", channels misnamed, were -Cz), ipsilateral to the left temporal stimulation (7 mA) applied at a 4.5 mm distance to Meyer's loop, in agreement with the visual functional neuroanatomy. Stimulations applied more remotely did not elicit any response (Video 2). Note that in Video 2, the right screen is the stack of the past SCEPs, each from about 30 averaged consecutive trials, where 2 consecutive past SCEPs can be seen, the first one being the one shown in Video 1. No decrease in VEP amplitude could be detected intraoperatively, independently of those of the electroretinogram; however, the patient exhibited a discrete superior homonym quadrantanopia 2 weeks post-surgery. Such limited visual field changes are usually not detect-

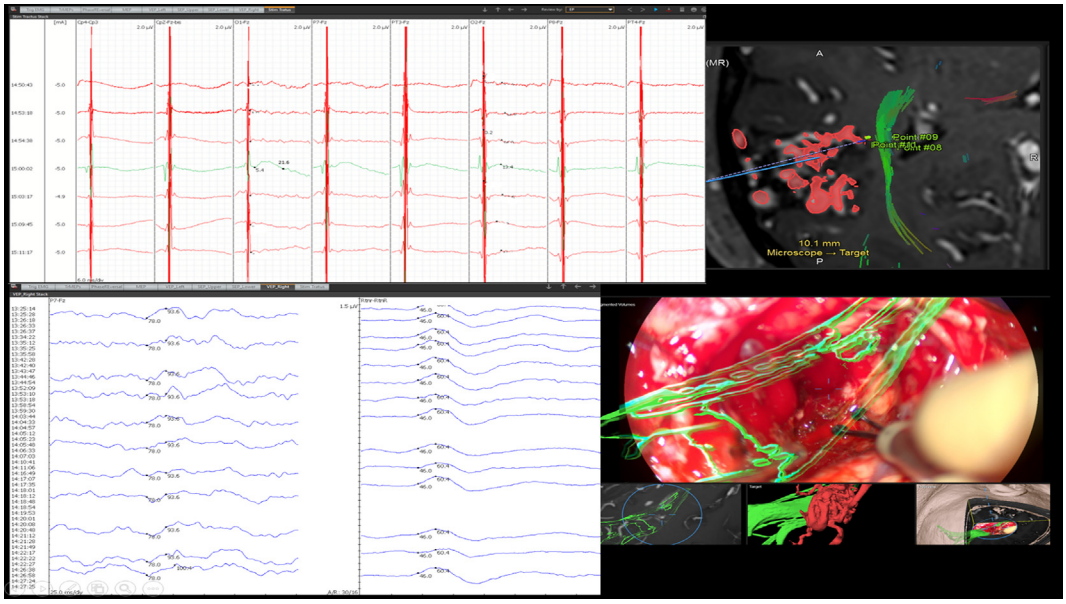

Fig. 1. Subcortico-cortical evoked potentials (SCEPs) observed during the surgery for a left temporo-occipital arteriovenous malformation (AVM). Upper right: Intra-operative sagittal navigation screenshots including in solid thin blue line the microscope optic axis and planned surgical reference trajectory (dotted blue line) with labeled stimulation sites (yellow dots), in patient P9 undergoing a left temporo-occipital resection of an AVM (red). Lower right: The bipolar stimulation probe can be seen in contact with the white matter at the edge of the optic radiation model, in green, simultaneously injected into the eyepiece of the microscope. Three insets immediately below: enhanced T1-weighted MPRAGE slice orthogonal to the optical microscope axis, volumetric rendering of the AVM (red), and microscope projection view in the patient's digital avatar. Upper left: The stimulation location point #11 evoked subcortico-cortical evoked potentials (SCEPs in green; every trace is the result of the average of about 30 trials) with P1 (5.4 ms) and P2 (21.6 ms) waveforms observed at the left occipital channel (green trace, "O1-Fz", channels misnamed were -Cz; abscissa: time scale [ms]). Note that the point 11 was the closest stimulated location to the optic radiation (i.e. 3 mm; in this single patient the distance was measured intraoperatively). The stimulation was performed at the end of resection. Lower left: Visual evoked potentials (VEPs) of the right eye, with left occipital recordings (left column) and right eye electroretinogram (right column), were performed (14 h16, 14 h18: temporary decrease, independent of that of the electroretinogram). (For interpretation of the references to colour in this figure legend, the reader is referred to the web version of this article.)

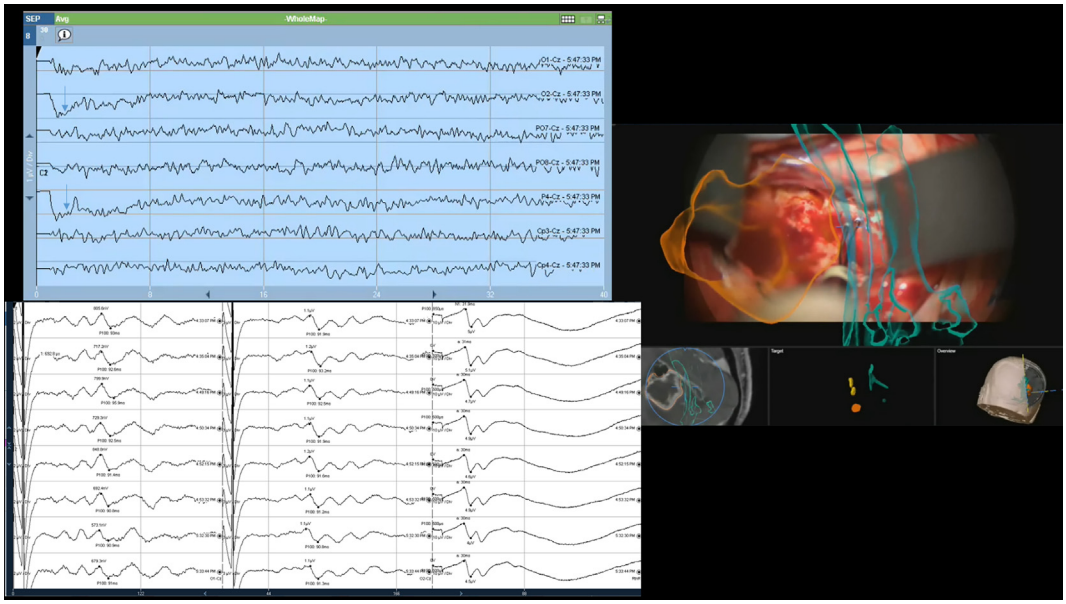

Fig. 2. Subcortico-cortical evoked potentials (SCEPs) observed during the surgery for a right parietal high grade glioblastoma. Right: The bipolar stimulation probe can be seen in contact with the white matter at the edge of the optic radiation model (green), simultaneously injected into the eyepiece of the microscope in patient P15, undergoing a right temporo-parietal resection of a glioblastoma (orange). Upper left: Subcortico-cortical evoked potentials (SCEPs) with P1 waveforms observed at the left occipital and parietal cortical channels (O2-Cz, P4-Cz), in response to the stimulation performed at the end of resection (average of 30 trials in this case). Lower left: Stable visual evoked potentials (VEPs) with occipital recordings and right eye electroretinogram (abscissa: time scale [ms]). (For interpretation of the references to colour in this figure legend, the reader is referred to the web version of this article.)

able by VEPs (Gutzwiller et al., 2018, Kodama et al., 2010, Sasaki et al., 2010).

In the other case of Meyer's loop stimulation, during temporo-mesial resection of a right hippocampal sclerosis (P1), no response could be detected, while the stimulation intensity was not higher than 3 mA for a distance to Meyer's loop of 6.2 mm according to the postoperative imaging, and no postoperative deterioration of the visual field was observed.

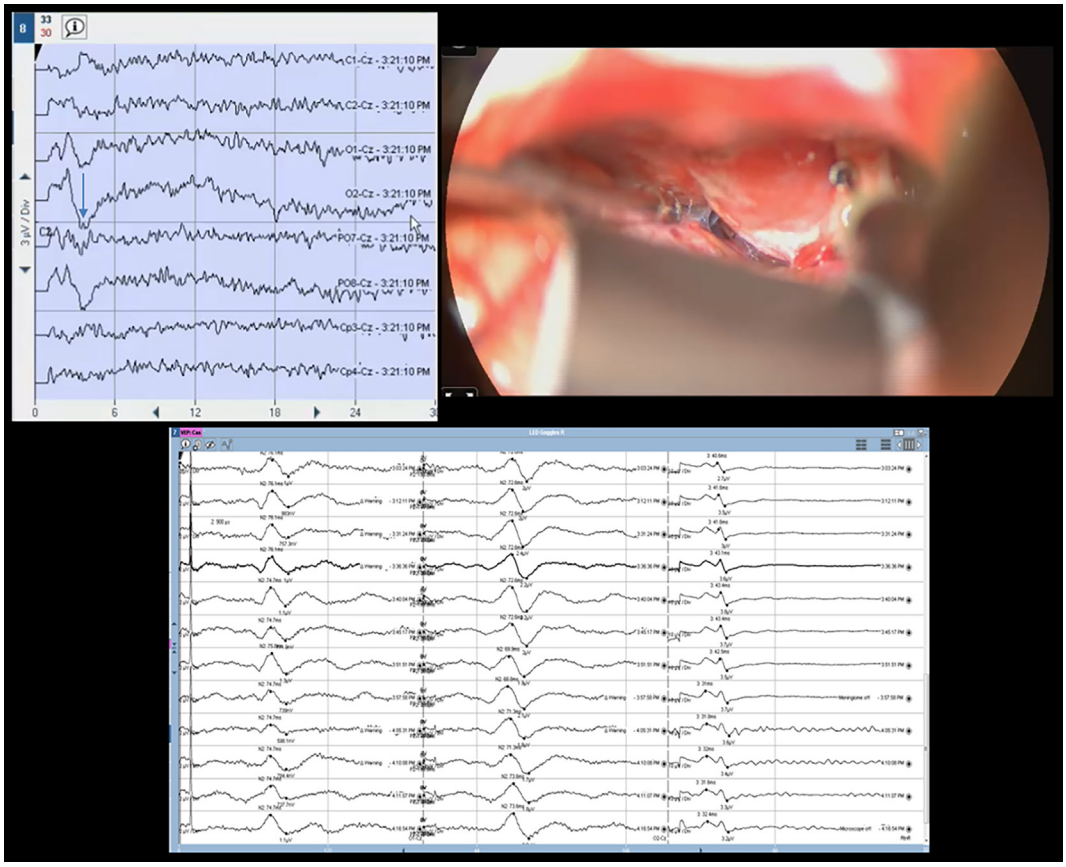

Fig. 3. Bipolar stimulation of the right optic nerve's lateral aspect in patient P18, just before resection of a sphenoidal meningioma. Upper left: Subcortico-cortical evoked potentials (SCEPs) with P1 waveforms (left) were observed bi-occipitally (O2-Cz > O1-Cz; for the average of 33 trials in this case) as well as on the right parieto-occipital electrode (P08-Cz). Upper right: The bipolar stimulation probe can be seen in contact with the right lateral optic nerve. Lower: Visual evoked potentials (VEPs) with bi-occipital recordings (O1-Cz, O2-Cz) were stable (abscissa: time scale [ms]).

Direct stimulation of the optic nerve (P10, P17, P18, Table 1) evoked a P1 waveform, observed bi-occipitally in agreement with the visual functional neuroanatomy, for the 2.5 to 3.5 mA stimulation range. As shown in Fig. 3, the bipolar stimulation of the right optic nerve's lateral aspect in patient P18 (2.5 mA) produced evoked potentials in the form of ipsilateral P1 responses (4.2 ms latency). Note that because of the surgical approach the right optic nerve was first exposed and stimulated just before the beginning of the resection and before the left optic nerve exposure. In agreement with the absence of intraoperative VEP changes, no significant visual field change was observed, except for a quadrantanopia in patient P10.

4. Discussion

In the present study, cortical responses evoked by subcortical electrical stimulation applied at various segments of the optic pathways were measured intraoperatively, during the resection of cerebral lesions under general anesthesia. To our knowledge, this is the first report of the application of such electrically evoked responses in the literature. Stimulation of the optic radiation evoked short latency P1 waveforms and occasionally middle latency P2 responses. No longer latency response was observed. No evoked potential could be recorded when the stimulation was applied further than a postoperatively determined distance of 4.5 mm from the closest visual path fibers. A high proximity of the stimulation with Meyer's loop or the optic radiation was generally associated with VEP declines and post-operative visual field alterations.

The short latency of the P1 waveform (i.e. 3.0–5.6 ms) is in accordance with the fact that a short distance separates the stimulation site and the occipital recording site, i.e. about 15 cm for optic nerve stimulation, 10 cm for temporal lobe stimulation and 5 cm for parietal stimulation. The short latency of the P1 response waveform (i.e. 3.0–5.6 ms) may be explained by the conduction along connecting myelinated fibers, which carry signals with a velocity of up to 30 m/s (Wang et al., 2008). These short latencies were hence in agreement with the distances between the stimulation location within the visual pathway and the primary cortex. Furthermore, the subcortical stimulation resulting in P1 responses could provoke an excitation of axons with very short conduction times, either from the optic nerve or the lateral geniculate nucleus that directly project to the motion-selective middle temporal area, a pathway involved in survival situations (Sincich et al., 2004), or from a fraction of the visual pathways that is free of synapses and where the velocity of signal propagation along myelinated fibers is particularly fast (Wang et al., 2008).

Electrical stimulation of the optic nerves was previously attempted and showed responses similar to the P2 response waveform observed in the present study (Benedicic and Bosnjak, 2011). The P2 responses obtained here (i.e. 15–21.6 ms, depending on the different sites of stimulation) were recorded either after direct or close stimulation (i.e. 2.1 mm) of the optic radiation. As in the study conducted by Benedicic and Bosnjak (2011) using extradural optic nerve stimulation, the stimulation intensities were relatively high, ranging from 5 to 8 mA. The latency waveforms P1 and P2 can

be compared to those reported for VEPs. The latency of the retinal responses was reported to be of a minimum of 20 ms, which can be attributed to the synapses between cones or rods and bipolar cells, and between bipolar cells and ganglion cells (McCulloch et al., 2015). Flash VEP waveforms, measured directly on the optic nerve of patients undergoing intracranial surgery, were even observed at the earliest at about 35 ms after the visual stimuli (Moller et al., 1987). The shortest latency of responses to flash stimulation in the optic tract was also measured at 22 ms (Yokoyama et al., 1999), while the latency was of 80 ms when recorded on the primary visual cortex (Ducati et al., 1988). The first occipital flash VEP waveform is usually observed at about 75 ms (Odom et al., 2016). The discrepancies found across these studies, all conducted in humans, were most probably due to differences in light exposure conditions, which considerably modify retinal excitation (McCulloch et al., 2015). The principal delay between the optic tract and occipital striatal cortical responses could reasonably be attributed to the synapses present in the lateral geniculate nucleus. Considering the short latency P1 waveform was attributed to the signal propagation along myelinated fibers, we state the hypothesis that the middle latency P2 waveform could be explained by partial activation of secondary visual cortices with direct and high intensity stimulation of the optic radiation.

The velocity of SCEPs is higher in comparison to diverse cortico-cortical evoked activities performed in awake patients, usually during invasive exploration of epilepsy (Matsuzaki et al., 2013, Trebaul et al., 2018). That can be explained by the fact that cortico-cortical evoked potentials excite portions of less myelinated fibers in the grey matter and involve synaptic excitation, which is a slower mechanism, while subcortical stimulation is directly delivered on highly myelinated white matter tracts. Again, under general anesthesia, the activation of secondary cortices was very limited, avoiding the masking of the shorter latency responses that could be neglected to the detriment of larger and longer latency responses observed in awake patients.

The P1 response waveform was not reported by Benedicic and Bosnjak (2011). Technical details related to signal processing could explain this lack of P1 observation. Indeed, to be able to measure short and middle latency responses, the high frequency component of the original recorded signals – where their energy is located – must be preserved, i.e. not attenuated by filtering. As Benedicic and Bosnjak (2011) did not include frequencies above 1000 Hz in their analyses, possible short latency signals could have been strongly attenuated, preventing their detection. On the other hand, in the present study, frequencies of up to 4000 Hz were preserved thanks to a high sampling frequency (20 kHz) using the intraoperative neuromonitoring systems, allowing P1 and P2 response waveforms to be observed. In addition, stimulation artifacts were limited thanks to bipolar stimulations applied with limited currents and voltages ($\leq$10 mA; $\leq$10 V). Applying these technical standards, similar intraoperative subcortical stimulations also evoked short and middle latency responses in the field of language mapping (Yamao et al., 2014).

Anyhow, the analyses of the distances from the visual pathway to the resection cavity support the idea that the P1 responses may be used to detect the visual pathways, since responses were observed for stimulations close to the optic radiation or to Meyer's loop, but not for more distant stimulations. The next step in the development of this technique would be to study the reproducibility of the SCEPs in particular with stimulation intensity and distance to the visual pathway. Improving the technique includes also developping a monopolar stimulation facilitatating dynamic continous mapping, necessary for ultrasonic aspirator stimulation or suction tool stimulation. One of the limitations of the study is that, all measurements of distances were done postoperatively based on the resection cavity on imaging and the DTI highlighting the optic radiation and Meyer's loop. No *rule of thumb* associating the stimulation intensity with the distance to the fibers, as that applied for motor mapping (Raabe et al., 2014), can be established yet, nor a threshold, wherein tissue resection would not pose any risk of visual impairment, similar to a safe motor threshold (Nossek et al., 2011, Plans et al., 2017, Prabhu et al., 2011, Sala and Lanteri, 2003, Seidel et al., 2013).

5. Conclusions

The direct stimulation of the optic nerve, Meyer's loop or of the optic radiation elicited short- and middle-latency cortical evoked responses. The short latency P1 evoked response waveform was in agreement with the velocity of signal propagation along intra-axial visual pathways. The middle latency P2 evoked response waveform could be attributed to the activation of secondary visual cortices after direct and high intensity stimulation of the optic radiation. At this stage of knowledge, no *rule of thumb* associating the stimulation intensity with the distance to the fibers – as that applied for motor mapping – can be established yet.

For neurosurgical ergonomics, in a next step, it would be valuable to obtain evoked responses resulting from stimulations performed via the surgical ultrasonic aspirator to continuously monitor the vicinity of the resection with respect to the visual tracts.

Appendix A. Supplementary data

Supplementary data to this article can be found online at https://doi.org/10.1016/j.clinph.2021.02.399.

References

Benedičič M, Bošnjak R. Intraoperative monitoring of the visual function using cortical potentials after electrical epidural stimulation of the optic nerve. Acta Neurochir 2011;153(10):1919–27.
Chen X, Weigel D, Ganslandt O, Buchfelder M, Nimsky C. Prediction of visual field deficits by diffusion tensor imaging in temporal lobe epilepsy surgery. NeuroImage 2009;45(2):286–97.
Ducati A, Fava E, Motti EDF. Neuronal generators of the visual evoked potentials: intracerebral recording in awake humans. Electroencephalogr Clin Neurophysiol 1988;71(2):89–99.
Duffau H. Intraoperative monitoring of visual function. Acta Neurochir 2011;153 (10):1929–30.
Duffau H, Velut S, Mitchell M-C, Gatignol P, Capelle L. Intra-operative mapping of the subcortical visual pathways using direct electrical stimulations. Acta Neurochir 2004;146(3):265–70.
Faust K, Vajkoczy P. Distinct displacements of the optic radiation based on tumor location revealed using preoperative diffusion tensor imaging. J Neurosurg 2016;124(5):1343–52.
Gepts E, Shafer SL, Camu F, Stanski DR, Woestenborghs R, Van Peer A, et al. Linearity of pharmacokinetics and model estimation of sufentanil. Anesthesiology 1995;83(6):1194–204.
Goodwin D. Homonymous hemianopia: challenges and solutions. Clin Ophthalmol 2014;8:1919–27.
Gras-Combe G, Moritz-Gasser S, Herbet G, Duffau H. Intraoperative subcortical electrical mapping of optic radiations in awake surgery for glioma involving visual pathways. J Neurosurg 2012;117(3):466–73.
Gutzwiller EM, Cabrilo I, Radovanovic I, Schaller K, Boex C. Intraoperative monitoring with visual evoked potentials for brain surgeries. J Neurosurg 2018:1–7.
Jeelani NU, Jindahra P, Tamber MS, Poon TL, Kabasele P, James-Galton M, et al. 'Hemispherical asymmetry in the Meyer's Loop': a prospective study of visual-field deficits in 105 cases undergoing anterior temporal lobe resection for epilepsy. J Neurol Neurosurg Psychiatry 2010;81(9):985–91.
Kodama K, Goto T, Sato A, Sakai K, Tanaka Y, Hongo K. Standard and limitation of intraoperative monitoring of the visual evoked potential. Acta Neurochir 2010;152(4):643–8.
Mandonnet E, Dadoun Y, Poisson I, Madadaki C, Froelich S, Lozeron P. Axono-cortical evoked potentials: a proof-of-concept study. Neurochirurgie 2016;62 (2):67–71.
Matsuzaki N, Juhász C, Asano E. Cortico-cortical evoked potentials and stimulation-elicited gamma activity preferentially propagate from lower- to higher-order visual areas. Clin Neurophysiol 2013;124(7):1290–6.

Mazerand E, Le Renard M, Hue S, Lemée J-M, Klinger E, Menei P. Intraoperative subcortical electrical mapping of the optic tract in awake surgery using a virtual reality headset. World Neurosurg 2017;97:424–30.
McCulloch DL, Marmor MF, Brigell MG, Hamilton R, Holder GE, Tzekov R, et al. ISCEV Standard for full-field clinical electroretinography (2015 update). Documenta ophthalmologica Adv Ophthalmol 2015;130(1):1–12.
Møller AR, Burgess JE, Sekhar LN. Recording compound action potentials from the optic nerve in man and monkeys. Electroencephalogr Clin Neurophysiol 1987;67(6):549–55.
Nossek E, Korn A, Shahar T, Kanner AA, Yaffe H, Marcovici D, et al. Intraoperative mapping and monitoring of the corticospinal tracts with neurophysiological assessment and 3-dimensional ultrasonography-based navigation. Clinical article. J Neurosurg 2011;114(3):738–46.
Odom JV, Bach M, Brigell M, Holder GE, McCulloch DL, Mizota A, et al. ISCEV standard for clinical visual evoked potentials: (2016 update). Documenta Ophthalmologica Adv Ophthalmol 2016;133(1):1–9.
Plans G, Fernandez-Conejero I, Rifa-Ros X, Fernandez-Coello A, Rossello A, Gabarros A. Evaluation of the high-frequency monopolar stimulation technique for mapping and monitoring the corticospinal tract in patients with supratentorial gliomas. a proposal for intraoperative management based on neurophysiological data analysis in a series of 92 patients. Neurosurgery 2017;81(4):585–94.
Prabhu SS, Gasco J, Tummala S, Weinberg JS, Rao G. Intraoperative magnetic resonance imaging-guided tractography with integrated monopolar subcortical functional mapping for resection of brain tumors. Clinical article. J Neurosurg 2011;114(3):719–26.
Raabe A, Beck J, Schucht P, Seidel K. Continuous dynamic mapping of the corticospinal tract during surgery of motor eloquent brain tumors: evaluation of a new method. J Neurosurg 2014;120(5):1015–24.
Sala F, Lanteri P. Brain surgery in motor areas: the invaluable assistance of intraoperative neurophysiological monitoring. J Neurosurg Sci 2003;47 (2):79–88.
Sasaki T, Itakura T, Suzuki K, Kasuya H, Munakata R, Muramatsu H, et al. Intraoperative monitoring of visual evoked potential: introduction of a clinically useful method. J Neurosurg 2010;112(2):273–84.
Schnider T, Minto C, Gambus P, Andresen C, Goodale D, Shafer S, et al. The influence of method of administration and covariates on the pharmacokinetics of propofol in adult volunteers. Anesthesiology 1998;88(5):1170–82.
Schnider TW, Minto CF, Shafer SL, Gambus PL, Andresen C, Goodale DB, et al. The influence of age on propofol pharmacodynamics. Anesthesiology 1999;90 (6):1502–1516..
Seidel K, Beck J, Stieglitz L, Schucht P, Raabe A. The warning-sign hierarchy between quantitative subcortical motor mapping and continuous motor evoked potential monitoring during resection of supratentorial brain tumors. J Neurosurg 2013;118(2):287–96.
Sincich LC, Park KF, Wohlgemuth MJ, Horton JC. Bypassing V1: a direct geniculate input to area MT. Nat Neurosci 2004;7(10):1123–8.
Smith JS, Chang EF, Lamborn KR, Chang SM, Prados MD, Cha S, et al. Role of extent of resection in the long-term outcome of low-grade hemispheric gliomas. J Clin Oncol 2008;26(8):1338–45.
Trebaul L, Deman P, Tuyisenge V, Jedynak M, Hugues E, Rudrauf D, et al. Probabilistic functional tractography of the human cortex revisited. NeuroImage 2018;181:414–29.
Wang SS, Shultz JR, Burish MJ, Harrison KH, Hof PR, Towns LC, et al. Functional trade-offs in white matter axonal scaling. J Neurosci 2008;28(15):4047–56.
Yamao Y, Matsumoto R, Kunieda T, Arakawa Y, Kobayashi K, Usami K, et al. Intraoperative dorsal language network mapping by using single-pulse electrical stimulation. Hum Brain Mapp 2014;35(9):4345–61.
Yamao Y, Suzuki K, Kunieda T, Matsumoto R, Arakawa Y, Nakae T, et al. Clinical impact of intraoperative CCEP monitoring in evaluating the dorsal language white matter pathway. Hum Brain Mapp 2017;38(4):1977–91.
Yeni SN, Tanriover N, Uyanik Ö, Ulu MO, Özkara Ç, Karaağaç N, et al. Visual field defects in selective amygdalohippocampectomy for hippocampal sclerosis: the fate of Meyer's loop during the transsylvian approach to the temporal horn. Neurosurgery 2008;63(3):507–15.
Yogarajah M, Focke NK, Bonelli S, Cercignani M, Acheson J, Parker GJM, et al. Defining Meyer's loop-temporal lobe resections, visual field deficits and diffusion tensor tractography. Brain : J Neurol 2009;132(6):1656–68.
Yokoyama T, Sugiyama K, Nishizawa S, Yokota N, Ohta S, Yamamoto S, Uemura K. Visual evoked oscillatory responses of the human optic tract. J Clin Neurophysiol 1999;16(4):391–6.
Zhang X, Kedar S, Lynn MJ, Newman NJ, Biousse V. Homonymous hemianopia in stroke. J Neuroophthalmol 2006;26(3):180–3.